Atomic layer deposition of HfO_2 on graphene from $HfCl_4$ and H_2O

Harry Alles[1,2], Jaan Aarik[1], Aleks Aidla[1], Aurelien Fay[2], Jekaterina Kozlova[1,3], Ahti Niilisk[1], Martti Pärs[1,*], Mihkel Rähn[1], Maciej Wiesner[2,4], Pertti Hakonen[2], and Väino Sammelselg[1,3]

[1]Institute of Physics, University of Tartu, Tartu, 51014, Estonia

[2]Low Temperature Laboratory, Aalto University, Espoo, P.O. Box 15100, Finland

[3]Institute of Chemistry, University of Tartu, Tartu, 50011, Estonia

[4]Faculty of Physics, Adam Mickiewicz University, Poznan, 61-614, Poland

Abstract

Atomic layer deposition of ultrathin HfO_2 on unmodified graphene from $HfCl_4$ and H_2O was investigated. Surface RMS roughness down to 0.5 nm was obtained for amorphous, 30 nm thick hafnia film grown at 180ºC. HfO_2 was deposited also in a two-step temperature process where the initial growth of about 1 nm at 170 ºC was continued up to 10–30 nm at 300 ºC. This process yielded uniform, monoclinic HfO_2 films with RMS roughness of 1.7 nm for 10–12 nm thick films and 2.5 nm for 30 nm thick films. Raman spectroscopy studies revealed that the deposition process caused compressive biaxial strain in graphene whereas no extra defects were generated. An 11 nm thick HfO_2 film deposited onto bilayer graphene reduced the electron mobility by less than 10% at the Dirac point and by 30–40% far away from it.

1. Introduction

Graphene, a single sheet of hexagonally bonded carbon atoms, is currently counted as one of the most promising materials that could allow the Moore's law to be tracked for several more years after the silicon road map ends. This is because graphene has high mobility of charge carriers at room temperature as it was demonstrated already in the very first experiments in 2004 [1]. Electronic transport properties of graphene have been investigated mostly for uncoated single- or few-layer sheets prepared by micromechanical cleaving of graphite or by decomposition of silicon carbide [2]. However, in order to develop real graphene-based electronic devices, one has to be able to prepare efficient top gates with ultra-thin high-k dielectrics on graphene. Recent progress in the preparation of wafer-scale graphene either synthesized by chemical vapor deposition [3–5] or by thermal treatment of SiC [2,6] has made this task even more important.

Atomic layer deposition (ALD) is probably the most suitable method for controlled deposition of ultrathin dielectric films with uniform thickness [7]. Unfortunately, the initiation of ALD on graphene is difficult due to the lack of dangling bonds on the graphene plane, which is similar to the surface of carbon nanotubes [8]. In the case of carbon nanotubes, the surface has been functionalized using nitrogen dioxide (NO_2) and trimethylaluminum ($Al[CH_3]_3$), and subsequently coated with Al_2O_3 by ALD [9]. Similarly Al_2O_3 has been deposited also on graphene [10].

Functionalization, however, can lead to severe degradation of transport properties of graphene [11]. For this reason there have been attempts to grow dielectrics (e.g. Al_2O_3 and HfO_2) directly on as-cleaved graphene and HOPG [12–14]. In most cases conventional H_2O-based ALD processes did not yield uniform metal oxide layers on these surfaces. Nevertheless, Meric *et al.* [15] were recently able to deposit HfO_2 directly on graphene using $[(CH_3)_2N]_4Hf$ and H_2O as precursors. According to

them the growth was most likely due to physisorption of a precursor on graphene at a very low substrate temperature (90 ºC). Unfortunately the surface of a HfO_2 film was noticeably rougher on graphene than on SiO_2. In addition, HfO_2 films, grown by ALD at low temperatures, have relatively small dielectric constants [16,17]. Thus, in order to obtain gate dielectrics with higher dielectric constant, it would be desirable to increase the deposition temperature.

In this paper we report on ALD of HfO_2 films on non-functionalized graphene surface grown from $HfCl_4$ and H_2O as precursors. By using a two-step process in which a HfO_2 seed layer was deposited at low temperature and the rest of the layer at high temperature, we succeeded to grow monoclinic HfO_2 films on graphene without producing additional defects in graphene. The significant compressive strain, which was detected in a single-layer graphene by Raman spectroscopy, indicated strong adhesion of HfO_2 to graphene.

2. Experimental

Our graphene samples were micromechanically extracted from natural (Madagascar) graphite and transferred onto Si substrates covered by 250 nm thick SiO_2 layer. The as-cleaved graphene flakes were characterized using Raman spectroscopy and atomic force microscopy (AFM) methods in order to determine the number and quality of graphene layers in those. For further experiments, samples with single- and bilayer graphene flakes were selected on the basis of these studies.

Onto one bilayer graphene sample on a highly doped Si substrate, we prepared Ti/Al/Ti electrodes with 10/50/5 nm layer thicknesses in order to perform electrical measurements. Six 0.3 μm wide electrodes with the distance of 0.3 μm between them were formed on a graphene stripe with the width of 1.3 μm using e-beam lift-off lithography and the electron beam evaporation methods. The bottom and top resists were made from polymethyl methacrylate and methacrylic acid

(PMMA/MAA) diluted in ethyl-lactate (10%) and PMMA diluted in anisole (3%), respectively. Both resist layers wer baked at 180 ºC for 5 min. Development was made in the solution of methyl isobutyl ketone and isopropyl alcohol (MIBK/IPA) for 10 s and in IPA for 20 s. After deposition of the metal layers the lift-off was done in a warm acetone.

The deposition of HfO_2 was studied in more detail on as-cleaved graphene. The HfO_2 films were deposited from $HfCl_4$ and H_2O in a flow-type low-pressure ALD reactor [18]. In order to synthesize HfO_2, an ALD cycle consisting of an $HfCl_4$ pulse (5 s in duration), purge of the reaction zone with N_2 (2 s), H_2O pulse (2 s) and another purge (5 s) was repeated until a film of required thickness was obtained. $HfCl_4$ was volatilized at a temperature of 140 ºC in the flow of N_2 carrier gas. The $HfCl_4$ pulses were formed by changing the flow direction of the carrier gas between the $HfCl_4$ source and reaction zone. The H_2O source was kept at the room temperature while the H_2O vapour was led to the reactor through a needle and solenoid valves, which controlled the precursor supply. At the reactor outlet, the partial pressure of H_2O was 5 Pa during an H_2O pulse while the N_2 pressure was approximately 250 Pa during the whole deposition process. The choice of precursor pressures as well as of pulse and purge durations was based on earlier real-time quartz crystal microbalance measurements [18,19] that demonstrated reliable self-limited character of the deposition at the process parameters used for deposition of HfO_2 on graphene in this work.

Three different temperature regimes were used for deposition of HfO_2 on the as-cleaved graphene samples. First, films with the thicknesses of 30–40 nm were deposited at 170–180 ºC. This temperature range is close to the lowest temperature, at which ALD of HfO_2 had been deposited from $HfCl_4$ [16,20]. At somewhat lower temperatures, unlimited condensation of $HfCl_4$ can take place on the substrate surface as the lowest temperatures ensuring sufficient evaporation rates of $HfCl_4$ for ALD range from 130 to 150 ºC [17–22]. Second, 10–30 nm thick films were grown in a two-step process: the growth was initiated at 170 ºC but after applying 10 ALD cycles the temperature was increased to 300 ºC and the growth was completed applying either 100–300 cycles.

As shown earlier, the film growth at lower temperatures should allow more uniform nucleation [21,22] but the concentration of the chlorine and hydrogen residues in the films grown from $HfCl_4$ and H_2O at temperatures below 225 ºC is high, exceeding 2-5% [17,20]. In the two-step process, we tried to achieve uniform nucleation at low temperature in the initial stage of deposition [22] and to grow HfO_2 with low impurity concentration and large dielectric constant on the top of the seed layer at a higher temperature. Using this approach, HfO_2 layer was also grown on the graphene sample that had electrodes for electrical measurements. For comparison, we deposited HfO_2 films on graphene by starting and completing the process at 300 ºC. Those films covered, however, the graphene flakes non-uniformly while the surface roughness exceeded that of the films grown in the two-step process by a factor of 2. For this reason, the films deposited at 300 ºC in a single-step process were not studied in more detail in this work.

After deposition of HfO_2 films the samples were again characterized by AFM and Raman spectroscopy techniques. In addition electron probe microanalysis (EPMA) method was applied to estimate the real thickness of HfO_2. Using the sample with electrodes, we measured differential AC-conductivity of graphene in a two-lead configuration at a frequency of 32 Hz and temperature of 4.2 K before and after the deposition of an 11 nm thick HfO_2 layer in a two-temperature ALD process. The highly doped Si substrate was used as a back gate in these measurements.

3. Results and discussion

The image depicted in Fig. 1a confirms that low deposition temperatures yield smooth HfO_2 films on graphene as the RMS surface roughness values of about δh_{rms} = 0.5 nm on graphene and δh_{rms} = 0.35 nm on SiO_2 were measured for a 30 nm thick HfO_2 films deposited at 180 ºC. For the films of the same thickness grown in the two-step process (Fig. 1b), these values reached ~2.5 and ~2 nm, respectively. It is worth noting in this context that markedly lower surface roughness (δh_{rms} = 1.7

nm on graphene and δh_{rms} = 0.9 nm on SiO_2) was measured for thinner (10–12 nm thick) HfO_2 films (Fig. 1c). This result indicates that rougher surfaces of films deposited in the two-step process compared to those of the films deposited at 180 ºC were due to crystallization of HfO_2 during the film growth at higher temperature rather than because of nucleation problems on the surface of graphene. At the same time, the surface roughness of 20–30 nm thick films grown at 300 ºC from the beginning of deposition process was as high as 5 nm on graphene and 2 nm on SiO_2. Thus, the seed layer deposited at 180 ºC allowed a marked reduction of the surface roughness of HfO_2 on graphene but caused no changes in the surface roughness on SiO_2. The absence of the effect of the seed layer on SiO_2 is an expected result because very uniform nucleation of HfO_2 can be obtained on oxidized Si at temperatures up to 300 ºC [21].

At the edge of a monolayer graphene flake, the AFM surface profile of the HfO_2 film deposited in the two-step process (Fig. 1d) very well corresponded to that of a single-layer graphene. Thus, the HfO_2 film grew with the same rate on graphene and SiO_2. The same result was obtained from EPMA studies. Consequently, application of the low-temperature seed layer allows minimization of the incubation period in the beginning of deposition on graphene. One should take into account, however, that although the seed layer obviously resulted in nucleation of the HfO_2 films on graphene without marked delay and in relatively smooth films grown in the two-step process, the surface of the films was still somewhat rougher on graphene compared to that on SiO_2. Therefore the deposition process parameters and thickness of the seed layer evidently need further optimization.

In order to determine the phase composition of HfO_2, we measured Raman scattering of the films on thick graphite flakes because strong scattering coming from Si substrate did not allow reliable characterization of HfO_2 on thin graphene flakes. We did not find any Raman peak for HfO_2 films deposited at 170–180 ºC. Hence, these films were amorphous. In the films deposited in the two-step growth process, we recorded scattering from monoclinic HfO_2 (Fig. 2). This conclusion is

based on the comparison of the Raman peaks measured in this work with a reference spectrum measured for a freestanding film that contained monoclinic HfO_2 as the only crystalline phase reliably determined by X-ray diffraction analysis [23].

Raman studies performed after deposition of HfO_2 indicated also a noticeable shift of the G and 2D bands of graphene compared to the positions of those recorded before HfO_2 deposition. Figure 3 shows the Raman spectra of a single-layer graphene sample taken at the same location before and after the deposition of an 11 nm thick HfO_2 layer in a two-step process. One can see from Fig. 3 that all Raman peaks of graphene recorded after deposition of HfO_2 are weaker than those recorded before HfO_2 deposition. In addition, the deposition of HfO_2 has resulted in an increase of the background intensity. Finally, and most importantly, the spectra clearly indicate blue-shifts of 9 and 22 cm^{-1} for the Raman G (at ~1580 cm^{-1}) and 2D (at ~2670 cm^{-1}) peaks, respectively, compared to the peak positions of uncoated graphene. Careful mapping of the whole area of a single-layer graphene (about 5 μm^2 in this particular sample) showed that the deviations of Raman peak positions did not exceed ±2.5 cm^{-1} for the G peak and ±5 cm^{-1} for the 2D peak. Therefore the blue-shifts observed cannot be because of edge effects [24] and/or possible inaccuracy of the positioning the laser beam at its initial location during Raman measurements. It is known that doping of graphene can also influence the positions of Raman peaks [25,26]. In this case, however, the shift of the 2D band should be smaller than [25] or comparable to [26] that of the G band. In addition, narrowing of the G band should accompany its blue-shift related to edge effects [24] and/or changes in the doping level [26]. In our case, on the contrary, the full width at half maximum of the G peak increases. On the basis of these data, one can conclude that compressive strain developed in graphene is the most probable reason for the blue-shifts of the Raman bands shown in Fig. 3.

Using the biaxial strain coefficient of –58 cm^{-1}/% for the Raman G mode and –144 cm^{-1}/% for the Raman 2D mode [27] and assuming elastic behavior of graphene, we estimated the compressive

strain to be ~0.15% in our single-layer graphene sample. A relatively large and *negativ*e thermal expansion coefficient of graphene (-7×10^{-6} K^{-1}at room temperature), which has recently been measured by Bao *et al.* [28], well explains the strain as the thermal expansion of HfO_2 is about the same magnitude but with the opposite (positive) sign [29]. We would also like to point out that our ALD process did not introduce additional defects into graphene as there was no measurable rise in the intensity of D (at ~1350 cm^{-1}) and D' (at ~1620 cm^{-1}) peaks in the Raman spectra.

Figure 4 displays differential conductivity, $\sigma = (L/W)\ (dI/dV_{ds})$, versus drain-source bias voltage V_{ds} measured at T = 4.2 K before and after the two-step growth process of an 11 nm thick HfO_2 film. The ALD deposition moved the charge neutrality point (CNP) from –39 V to +30 V in V_g but, nevertheless, the *I-V* characteristics did not change much at CNP (at V_g^{CNP}). A comparison of σ before and after ALD deposition indicates that the electron mobility μ ~ 2000 cm^2/Vs of the sheet was reduced by less than 10% at CNP and by 30–40% far away from it (at $\Delta V_g = V_g - V_g^{CNP} = 23$ V). The electron mobility μ was estimated from the relationship $\sigma = n\ e\ \mu$, where n is the charge carrier density and e is the electron charge. The charge density can be calculated from the formula $n = C_g\ V_g\ /e$ where C_g is the gate capacitance per surface area and V_g is the gate voltage. Using the plane capacitance model the value of C_g was estimated to be 180 aF/μm^2. In our sample, the spacing between two contacts (300 nm) is close to the SiO_2 thickness (250 nm). In that case, the electric field from the back gate is screened by the contacts and the gate capacitance is lower than estimated from the plane capacitance model. Consequently, the mobility of 2000 cm^2/Vs, calculated by us, can be underestimated. However, this mobility value is very close to the value observed by Geim et al. [30] for a bilayer graphene.

We also observed that the "Dirac point" moved from V_g = +30 V to +10 V in subsequent bias and gate voltage scans. This shift must be related to the loading of charge traps in the ALD coating, since such behavior was much weaker without HfO_2. The width of the "conductance dip" at CNP

around zero bias (for example, width ΔV at $\sigma = 10\ G_0$) is about 30% wider with the ALD coating. Finally, the asymptotic level of conductivity seems to be larger with HfO_2 than without it, when V_g is tuned far away from CNP. This might be an indication of improved, annealed contact conditions between graphene and metal electrode as the major part of the ALD process was done at $T = 300$ ºC.

4. Conclusions

We have demonstrated in this work that HfO_2 films can be successfully grown on non-functionalized graphene by ALD using $HfCl_4$ and H_2O as the precursors. Surface RMS roughness down to 0.5 nm was obtained for 30 nm thick amorphous films deposited on graphene at 180 ºC. By using a uniform, 1 nm thick seed layer produced at 170 ºC, and continuing at a higher temperature (300 ºC), crystalline HfO_2 films were grown on graphene. The films obtained were relatively smooth and grew with the same rate on graphene and SiO_2. Raman spectroscopy studies of a single-layer graphene revealed no generation of defects in graphene during the ALD process. However, we found that this kind of procedure leads to compressive strain in graphene because of the marked difference in thermal expansion coefficients of graphene and HfO_2. The conductivity measurements of a bilayer graphene sample at 4.2 K indicated that the electron mobility was reduced by less than 40% due to the coating of graphene with an HfO_2 film in a two-step process. Consequently, the two-step process is applicable for preparation of high-k gate dielectrics for top gates in graphene devices.

Acknowledgements

The authors would like to thank M. Paalanen and I. Sildos for fruitful discussions and for granting access to the experimental facilities needed for preparation and characterization of graphene. We are also thankful to R. Danneau and J. Wengler for their contributions at early stages of the work and Jelena Asari for EPMA measurements. This research was carried out with the financial support

from Estonian Science Foundation (Grants No. 6651, 6999 and 7845), and Estonian Ministry of Education and Research (targeted project SF0180046s07). One author (HA) also acknowledges the support from European Social fund (Grant MTT1). The work at LTL was supported by the Academy of Finland, EU contract FP6-IST-021285-2 (CARDEQ), and the NANOSYSTEMS project with Nokia Research Center.

References

*Present address: Universität Bayreuth, Lehrstuhl Experimentalphysik IV 95440 Bayreuth, Germany

[1] K.S. Novoselov et al., Science 306**,** 666 (2004)

[2] A.K. Geim, K.S. Novoselov, Nature Mater. 6 183 (2007)

[3] K.S. Kim et al., Nature 457, 706 (2009)

[4] A. Reina et al., Nano Lett. 9, 30 (2009)

[5] X.Li et al., Science 324, 1312 (2009)

[6] J. Kedzierski et al., IEEE Trans. Electron Devices 8, 2078 (2008)

[7] R.L. Puurunen, J. Appl. Phys. 97, 121301 (2005)

[8] A. Javey et al., Nano Lett. 4, 1319 (2004)

[9] D.B. Farmer, R.G. Gordon, Nano Lett. 6 699 (2006)

[10] J.R. Williams, L. DiCarlo and C.M. Marcus, Science 317, 638 (2007)

[11] Y.-M. Lin et al., Nano Lett. 9, 422 (2009)

[12] B. Lee et al., Appl. Phys. Lett. 92, 203102 (2008)

[13] X. Wang, S.M. Tabakman, H. Dai, J. Am. Chem. Soc. 130, 8152 (2008)

[14] Y. Xuan et al., Appl. Phys. Lett. 92, 013101 (2008)

[15] I. Meric et al., Nature Nanotechnol. 3, 654 (2008)

[16] G. Scarel et al., Mater. Sci. Eng. B 109, 11 (2004)

[17] K. Kukli et al., J. Appl. Phys. 96, 5298 (2004)

[18] J. Aarik et al., J. Cryst. Growth 220, 105 (2000)

[19] J. Aarik et al., Appl Surf. Sci. 252, 5723 (2006)

[20] J. Aarik et al., Thin Solid Films 340, 110 (1999)

[21] J. Aarik et al., Appl. Surf. Sci. 230, 292 (2004)

[22] K. Kukli et al., Thin Solid Films 479, 1 (2005)

[23] S.N. Tkachev et al., J. Mater. Sci. 40, 4293 (2005)

[24] C. Casiraghi et al., Appl. Phys. Lett. 91, 233108 (2007)

[25] A. Das et al., Nature Nanotechnol. 3, 210 (2008)

[26] Z. Ni et al., Nano Res. 1, 273 (2008)

[27] T.M.G. Mohiuddin et al., Phys. Rev. B 79, 205433 (2009)

[28] W. Bao et al., Nature Nanotechnol. 4, 562 (2009)

[29] J. Wang J, H.P. Li, R. Stevens, J. Mater. Sci. 27, 5397 (1992)

[30] A. Geim et al., Phys. Rev. Lett. 100, 016602 (2008)

Figure Captions

Figure 1. (color online) AFM images of HfO_2 films deposited on top of graphene flakes (a) at 180 ºC, and (b,c) in the two-step (170/300 ºC) growth process. RMS surface roughness values are (a) < 0.5 nm on graphene for a 30 nm thick film, (b) ~2.5 nm on graphene for a 30

nm thick film and (c) 1.7 nm on graphene and 0.9 nm on SiO_2 for an 11 nm thick film. (d) AFM height profile of an 11 nm thick HfO_2 film grown in the two-step process and measured at the edge of a graphene flake along the line A-A shown in panel (c). Scan areas are 1 x 1 μm^2.

Figure 2. Raman spectrum of a 30 nm thick monoclinic HfO_2 film deposited in the two-step growth process (170/300 ºC) on the top of a graphite flake (upper curve). For comparison, a reference spectrum of a free-standing monoclinic HfO_2 film is shown by the lower curve. The monoclinic structure of the latter film has been determined by X-ray diffraction analysis [23].

Figure 3. Raman spectra of a single-layer graphene sample taken at the same point (a) before and (b) after the deposition of an 11 nm thick HfO_2 layer in the two-step (170/300 ºC) growth process.

Figure 4. (color online) Differential conductivity $\sigma = (L/W)\ (dI/dV_{ds})$ versus drain-source bias voltage V_{ds} for a bilayer graphene sample (length L = 0.3 μm, width W = 1.3 μm), measured at T = 4.2 K before and after the deposition of an 11 nm thick HfO_2 film using the two-step (170/300 ºC) growth process; ΔV_g denotes the back gate voltage offset from the charge neutrality point (“Dirac point”).

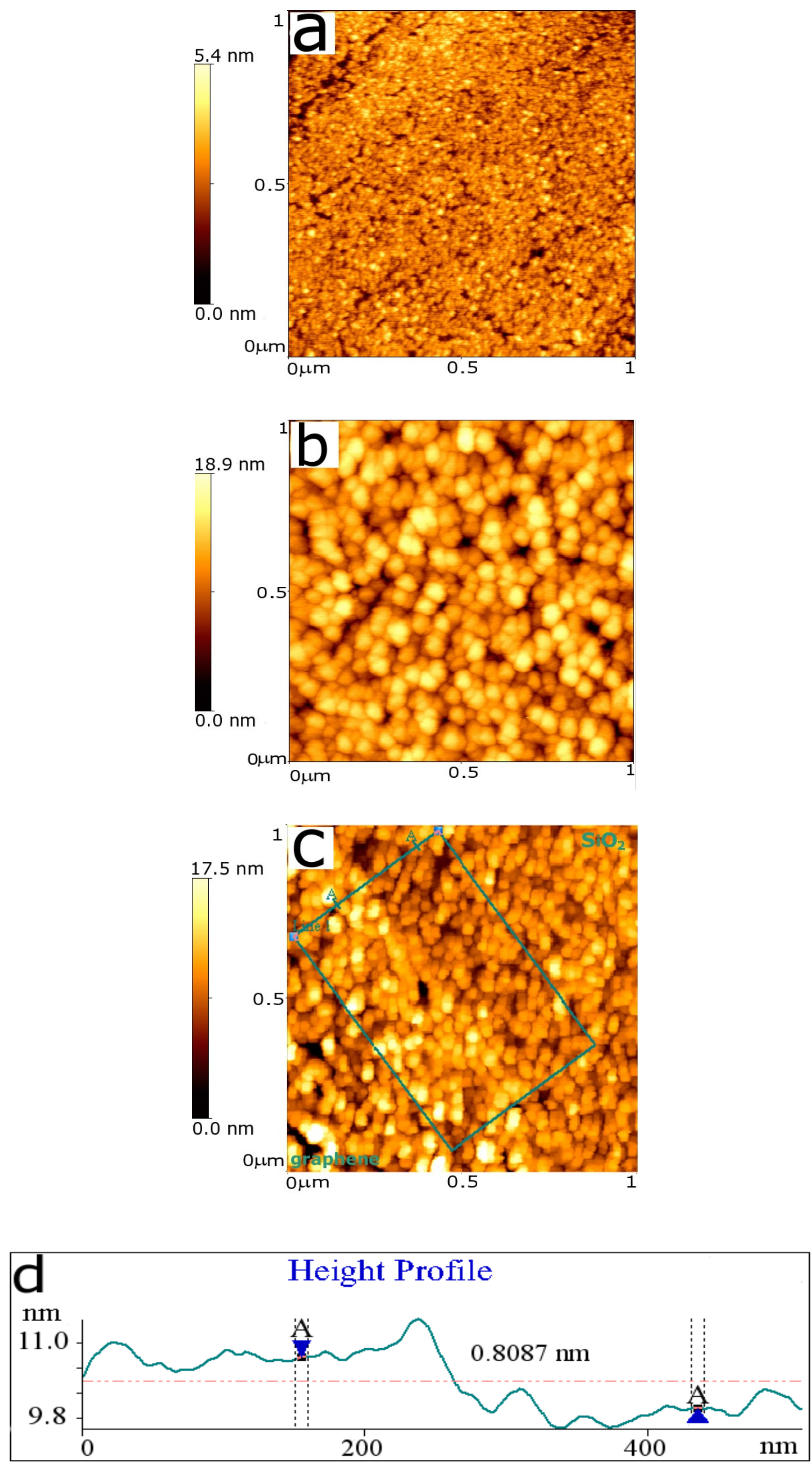

Figure 1

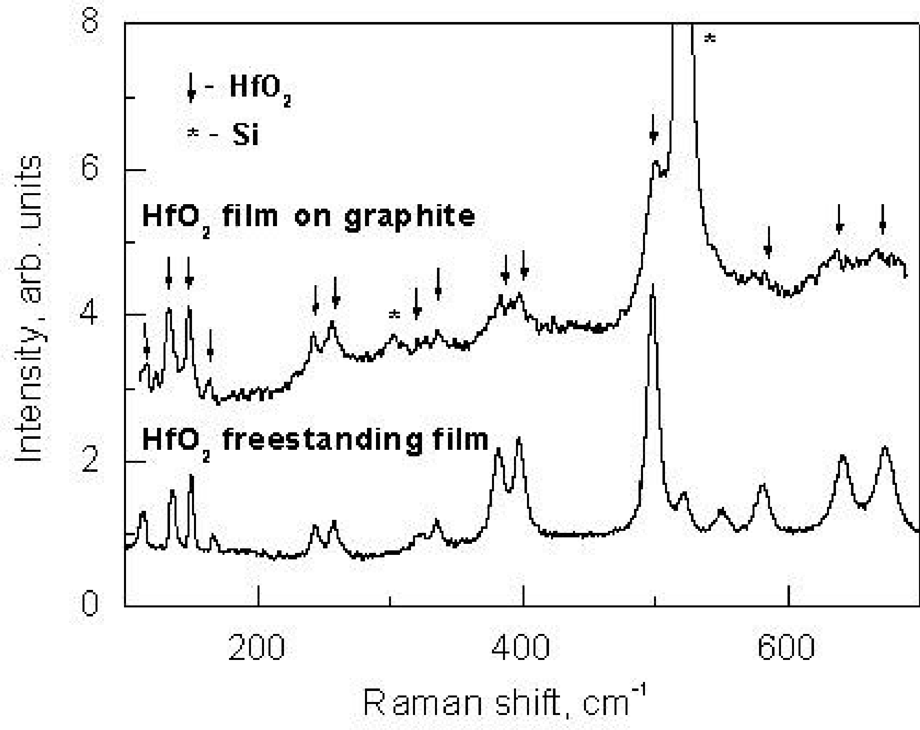

Figure 2

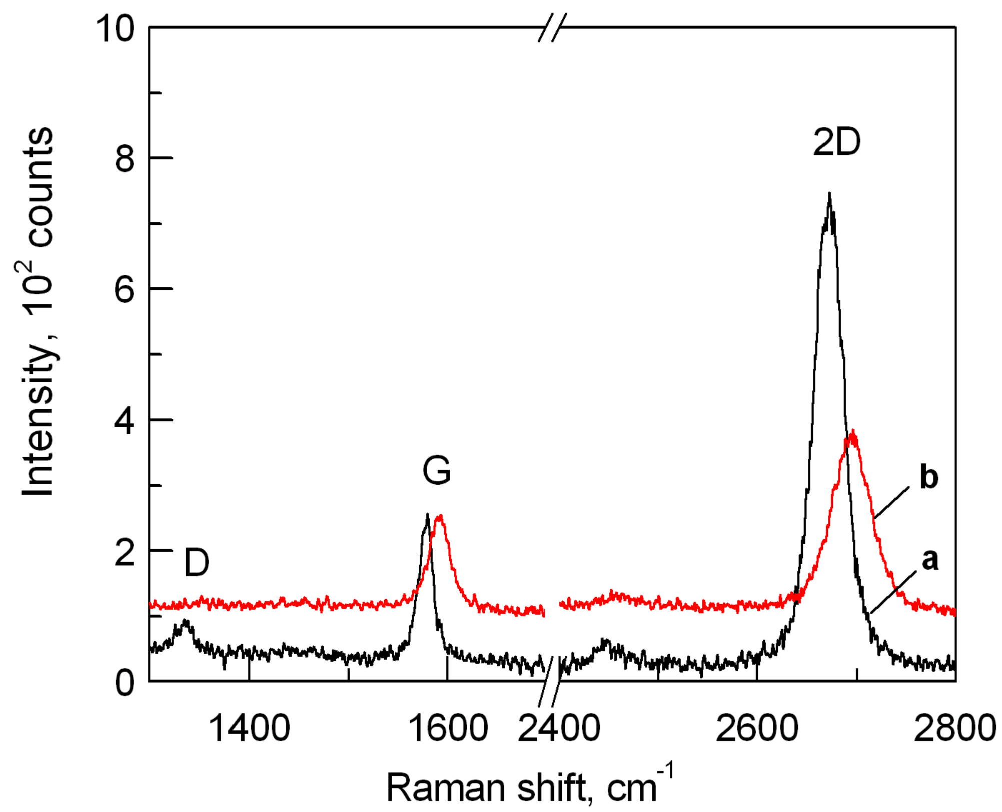

Figure 3

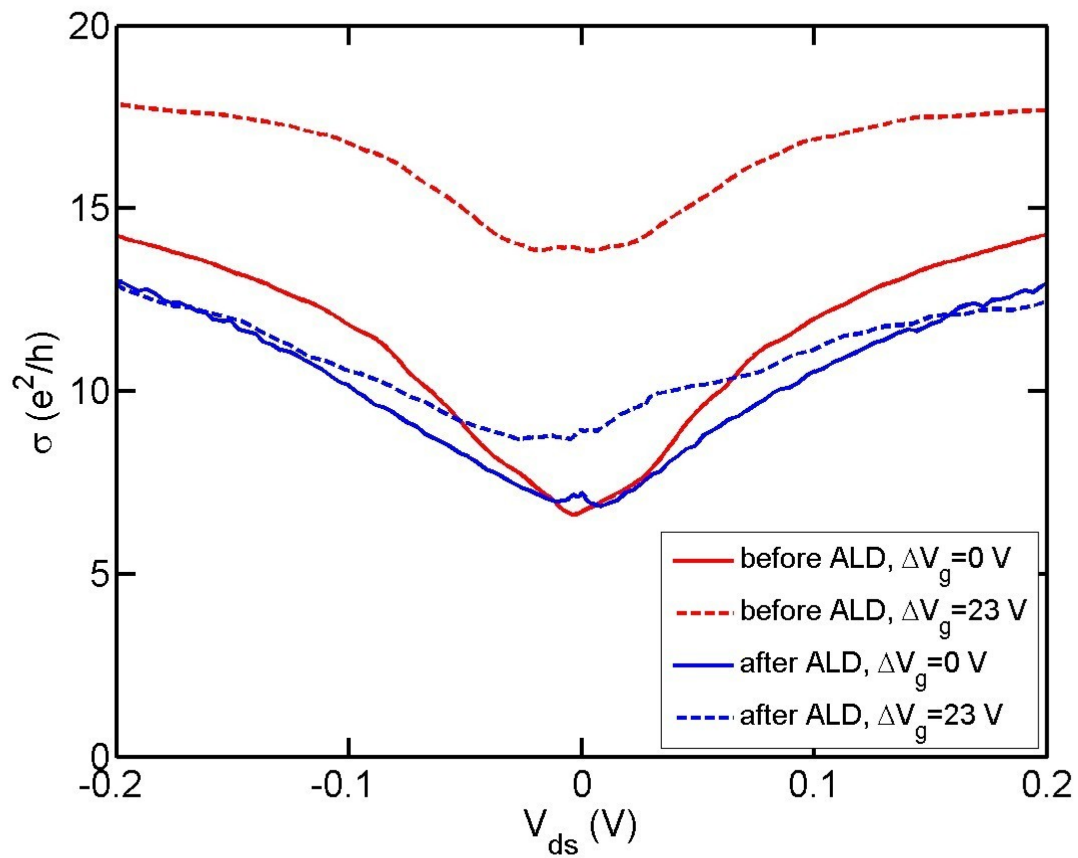

Figure 4